SIGNAL TRANSDUCTION

Opposing effects of Elk-1 multisite phosphorylation shape its response to ERK activation

Anastasia Mylona,[1]* Francois Xavier Theillet,[2]† Charles Foster,[1] Tammy M. Cheng,[3] Francesc Miralles,[1,4] Paul A. Bates,[3] Philipp Selenko,[2] Richard Treisman[1]‡

Multisite phosphorylation regulates many transcription factors, including the serum response factor partner Elk-1. Phosphorylation of the transcriptional activation domain (TAD) of Elk-1 by the protein kinase ERK at multiple sites potentiates recruitment of the Mediator transcriptional coactivator complex and transcriptional activation, but the roles of individual phosphorylation events had remained unclear. Using time-resolved nuclear magnetic resonance spectroscopy, we found that ERK2 phosphorylation proceeds at markedly different rates at eight TAD sites in vitro, which we classified as fast, intermediate, and slow. Mutagenesis experiments showed that phosphorylation of fast and intermediate sites promoted Mediator interaction and transcriptional activation, whereas modification of slow sites counteracted both functions, thereby limiting Elk-1 output. Progressive Elk-1 phosphorylation thus ensures a self-limiting response to ERK activation, which occurs independently of antagonizing phosphatase activity.

Multisite protein phosphorylation increases the complexity of functional signaling outputs that can be generated from single protein kinase inputs. It can set thresholds for activity or transform graded signals into switch like responses (*1 4*). Many transcription factors and their interacting regulatory proteins are subject to multisite phosphorylation, which allows distinct aspects of protein function including protein turnover, nuclear import and export, and specific protein interactions to be controlled independently (*5*). However, in general, the dynamics and functional roles of individual phosphorylation events are incompletely understood.

The ternary complex factor (TCF) subfamily of Ets domain transcription factors, consisting of Elk 1, SAP 1, and Net, provides an example of multisite phosphorylation in transcriptional activation. TCFs, together with their partner protein SRF, function in many biological processes by coupling SRF target genes to mitogen activated protein kinase (MAP kinase) signaling (*5*). Mitogenic and stress stimuli induce phosphorylation of TCF C terminal transcriptional activation domains (TADs) at multiple S/T P (Ser or Thr Pro) phosphorylation sequences, of which eight are conserved across the family (Fig. 1A and fig. S1) (*6 11*). Two MAP kinase docking sites, the D box and the Phe Gln Phe Pro (FQFP) motif, control phosphorylation of these sites (*12 15*). Multisite phosphorylation triggers transcriptional activation by TCFs, facilitating their interaction with the Mediator transcriptional coactivator complex (*16 19*), but the kinetics with which the different sites are phosphorylated, and whether they serve distinct functions, remain unclear.

To obtain atomic resolution insights into phosphorylation of the Elk 1 TAD, we used nuclear magnetic resonance (NMR) spectroscopy (*20*) to monitor its modification by recombinant ERK2 in vitro (Fig. 1B and fig. S2A). Time resolved NMR experiments revealed that each phosphorylation proceeded efficiently but at markedly different rates. Phosphorylation of Thr^{369} and Ser^{384}, which flank the central Phe Trp (FW) motif implicated in Mediator interaction (*18*), occurred faster than

[1]Signalling and Transcription Laboratory, Francis Crick Institute, Lincoln's Inn Fields Laboratory, London WC2A 3LY, UK. [2]In Cell NMR Laboratory, Department of NMR Supported Structural Biology, Leibniz Institute of Molecular Pharmacology (FMP Berlin), Berlin, Germany. [3]Biomolecular Modelling Laboratory, Francis Crick Institute, Lincoln's Inn Fields Laboratory, London WC2A 3LY, UK. [4]Molecular & Clinical Sciences Research Institute, St. George's, University of London, London SW17 ORE, UK.
*Present address: AM, Faculty of Life Sciences & Medicine, Guy's Campus, Kings' College London, London SE1 1UL, UK. †Present address: F XT, Institute of Integrative Biology of the Cell (I2BC), CNRS/CEA/Paris Saclay University, 91191 Gif sur Yvette, France.
‡Corresponding author. Email: richard.treisman@crick.ac.uk

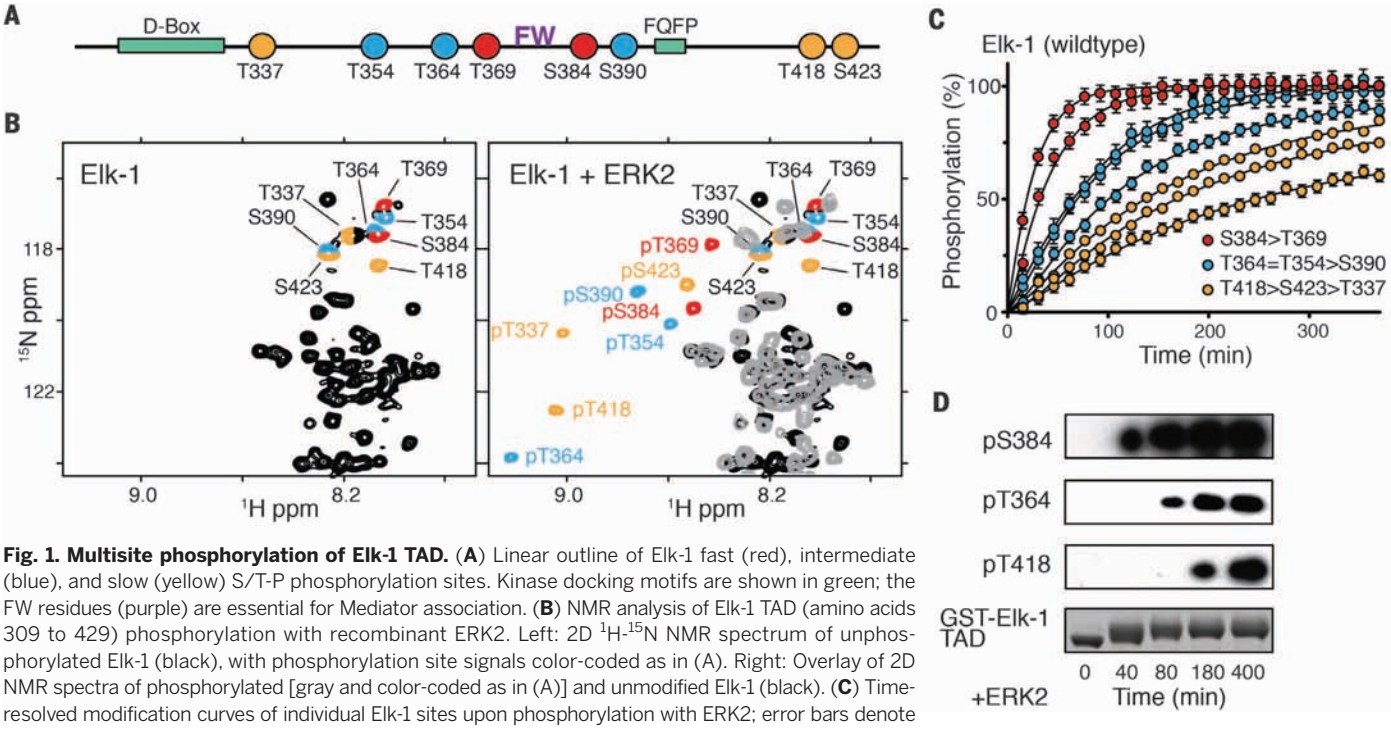

Fig. 1. Multisite phosphorylation of Elk-1 TAD. (**A**) Linear outline of Elk-1 fast (red), intermediate (blue), and slow (yellow) S/T-P phosphorylation sites. Kinase docking motifs are shown in green; the FW residues (purple) are essential for Mediator association. (**B**) NMR analysis of Elk-1 TAD (amino acids 309 to 429) phosphorylation with recombinant ERK2. Left: 2D ^{1}H-^{15}N NMR spectrum of unphosphorylated Elk-1 (black), with phosphorylation site signals color-coded as in (A). Right: Overlay of 2D NMR spectra of phosphorylated [gray and color-coded as in (A)] and unmodified Elk-1 (black). (**C**) Time-resolved modification curves of individual Elk-1 sites upon phosphorylation with ERK2; error bars denote differences between replicate experiments on two independent samples. (**D**) Time-course Western blot of GST–Elk-1 TAD phosphorylation and phosphorylation site–specific antibody detection.

modification of Thr^{354}, Thr^{364}, and Ser^{390}, whereas residues Thr^{418}, Ser^{423}, and Thr^{337} were modified more slowly (Fig. 1C), which we confirmed by immunoblotting (Fig. 1D). Chemical shift anal ysis (Cα, Cβ) showed no stable secondary struc ture elements in unmodified or phosphorylated Elk 1 TAD (fig. S2B).

As a first step toward understanding the basis for the phosphorylation sites' differential kinetic behavior, we devised a reaction model based on Michaelis Menten enzyme kinetics. To simplify the mathematical treatment, we grouped Elk 1 sites into three classes: fast (Thr^{369} and Ser^{384}), inter mediate (Thr^{354}, Thr^{364}, and Ser^{390}), and slow (Thr^{337}, Thr^{418}, and Ser^{423}). We assumed that ERK2 phos phorylation is distributive, that enzymatic rate constants (k_{cat}) are similar for all sites, and that the different sites have relative affinities for ERK2 modeled by increasing Michaelis Menten constants ($K_M^{Fast} < K_M^{Int} < K_M^{Slow}$) (Fig. 2A and fig. S3A) (*20*). This model, which recapitulated the measured kinetics of in vitro Elk 1 phospho rylation well (Fig. 2B), predicted that removal of fast or intermediate sites should increase the phosphorylation rates of other sites. To test this idea, we analyzed the phosphorylation kinetics of Elk 1 TAD mutants in which we substituted all fast or intermediate phosphoacceptor residues with alanines (Elk 1F: Thr^{369} → Ala, Ser^{384} → Ala; Elk 1I: Thr^{354} → Ala, Thr^{364} → Ala, Ser^{390} → Ala) (Fig. 2A). In the fast site mutant Elk 1F, phosphorylation rates of intermediate and slow sites increased, whereas those of the fast and slow sites increased in the intermediate site mutant Elk 1I; in both cases, the altered kinetics fit well with those predicted by the model (Fig. 2B and fig. S3B). Thus, even the fast sites are not phosphory lated at the maximum possible rate in the wild type protein. Moreover, phosphorylation of an Elk 1 TAD mutant in which Thr^{369} and Ser^{384} were replaced with aspartates was similar to Elk 1F, excluding the possibility that fast site phos phorylation primes later modification events (fig. S3B).

To gain more insight into the factors affecting individual sites' phosphorylation kinetics, we as sessed the role played by primary sequence. To do this, we exchanged the sequences surrounding the fast Thr^{369} and slow Ser^{423} sites. This also effectively exchanged their reactivities, which sug gests that these sites' phosphorylation rates reflect their position relative to ERK docking sequences, rather than intrinsic differences in reactivity (Fig. 2C). We therefore examined the contributions of the D box and FQFP ERK docking motifs to each site's phosphorylation kinetics. Deletion of the D box decreased the rates of Thr^{337}, Thr^{354}, Thr^{364}, and Thr^{369} phosphorylation but increased the rates of Ser^{390}, Thr^{418}, and Ser^{423} modification (Fig. 2D). In contrast, deletion of the FQFP motif decreased the rate of Ser^{384} phosphorylation but enhanced modification of intermediate sites, including ad jacent Ser^{390}, with no effect on the C terminal sites (Fig. 2D). Thus, the ERK docking motifs dif ferentially affect each phosphorylation site's com petitive behavior. Previous studies showed that Elk 1 TAD phosphorylation by JNK and p38

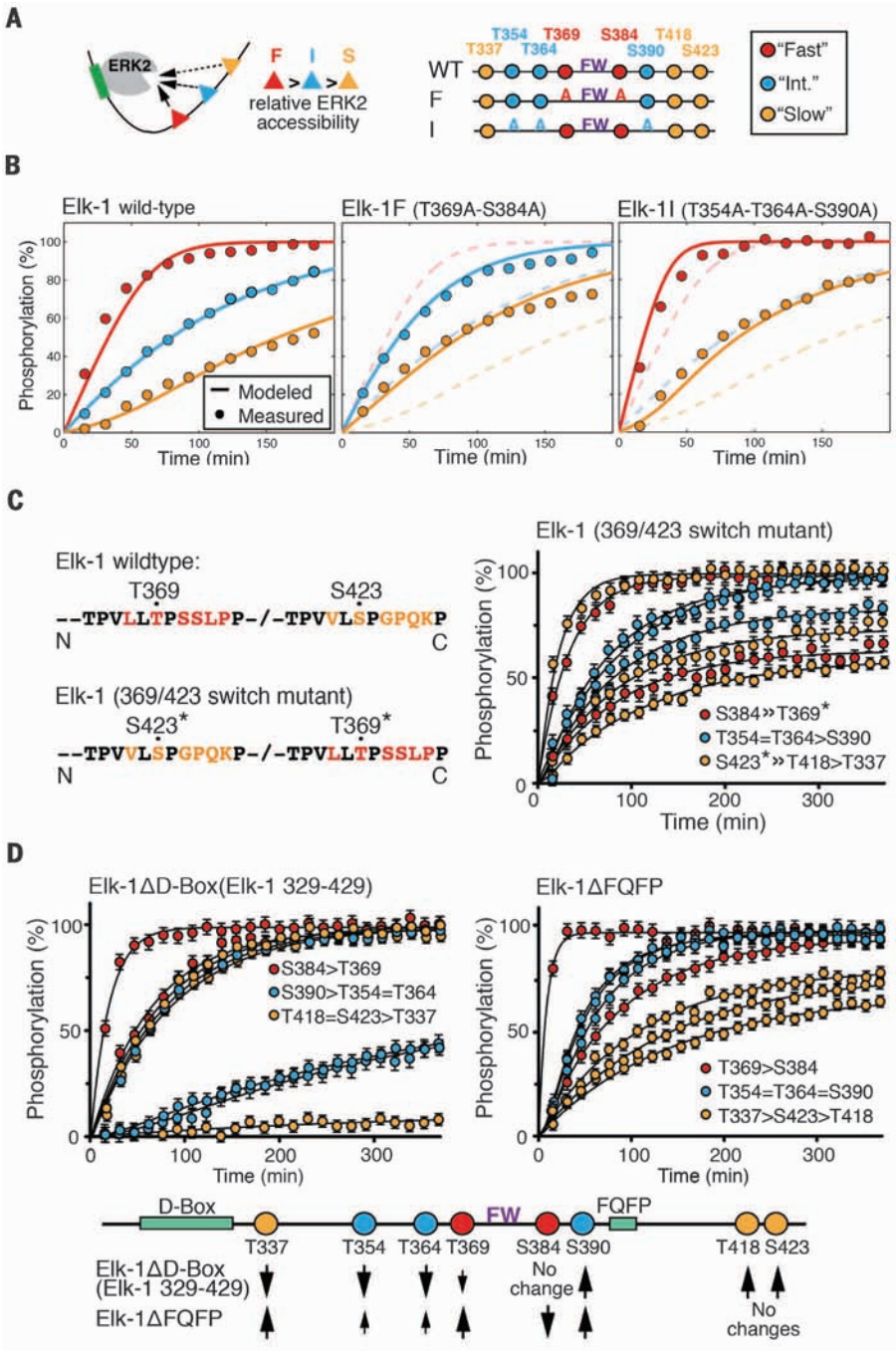

Fig. 2. Phosphorylation kinetics of Elk-1 TAD mutants. (**A**) Outline of analyzed Elk-1 TAD mutants. Substrate sites were classified as fast (red), intermediate (blue), or slow (yellow) for model calculations. (**B**) Left: Comparison of averaged measured data points of wild-type Elk-1 TAD fast-, intermediate-, and slow-site phosphorylation by ERK2 (circles) with calculated rates according to the competitive inhibition model (solid lines). Center: Fast-site alanine-substituted Elk-1 TAD (Elk-1F); dashed lines show wild-type Elk-1 TAD for comparison. Right: Intermediate-site alanine-substituted Elk-1 TAD (Elk-1I); dashed lines show wild-type Elk-1 TAD for comparison. (**C**) Time-resolved modification curves (right) of the Elk-1 369/423 switch mutant (left). Amino acid abbreviations: G, Gly; K, Lys; L, Leu; P, Pro; Q, Gln; S, Ser; T, Thr; V, Val. Error bars denote differences between replicate experiments on two independent samples. (**D**) Time-resolved modification curves of ERK docking-site mutants Elk-1ΔD-box (left) and Elk-1ΔFQFP (right), presented as in (C). Effects of D-box and FQFP site deletions on Elk-1 TAD phosphorylation rates are summarized below.

MAP kinases differs from phosphorylation by ERK (*10*, *21*, *24*) and that this reflects differences in their docking interactions (*12*, *14*, *15*, *25*). In deed, these kinases exhibited site preferences and phosphorylation rates that were distinct from that of ERK2 (fig. S3C). Taken together,

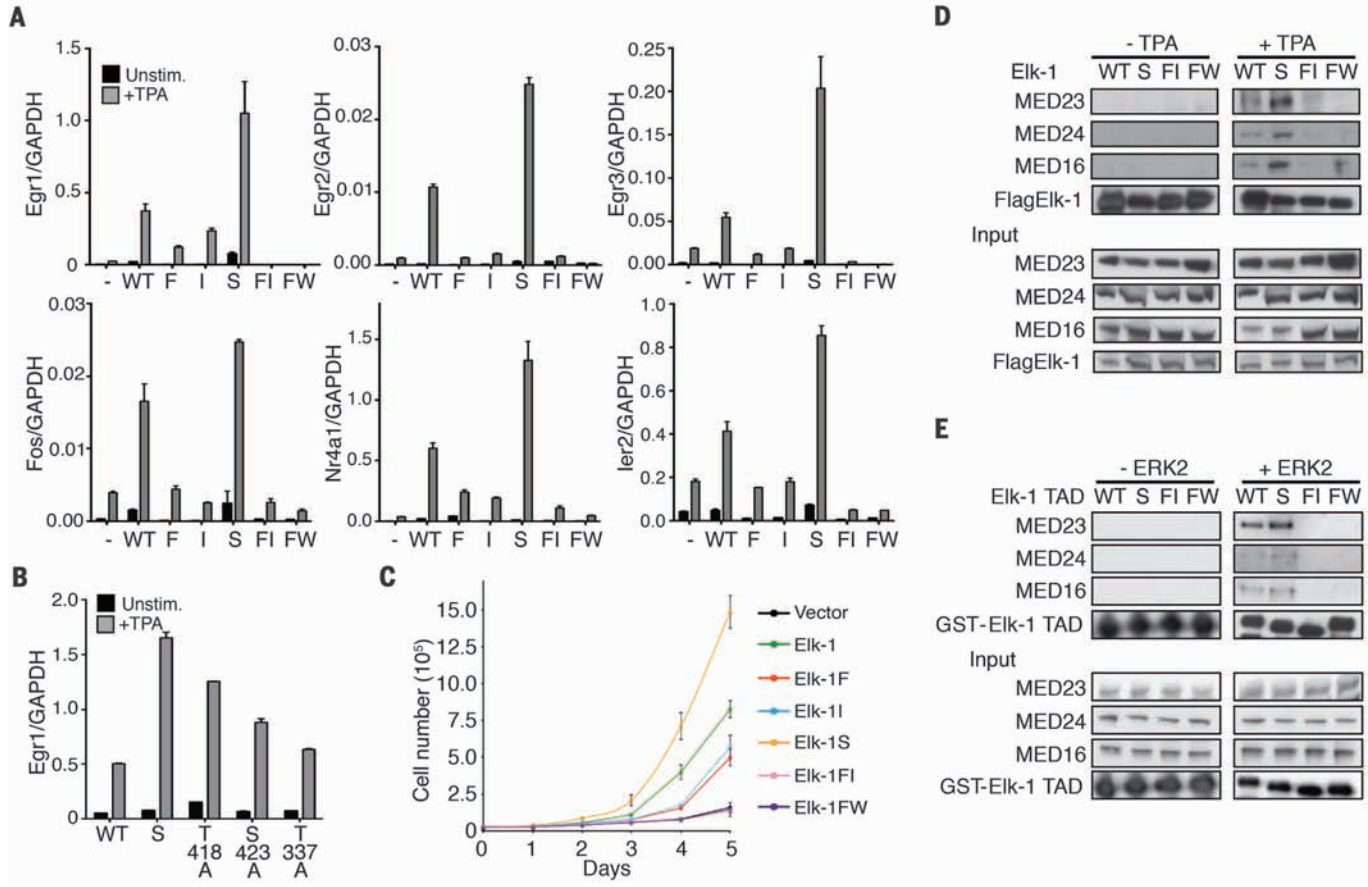

Fig. 3. Effects of Elk-1 TAD mutations on TCF target gene expression, cell proliferation, and Mediator bind ng. (**A**) Quantitative reverse transcription polymerase chain reaction (qRT-PCR) analysis of TCF target gene transcription in reconstituted TKO MEFs. Cells were reconstituted with wild-type mouse Elk-1 (WT) or fast-site (F), intermediate-site (I), slow-site (S), fast- and intermediate-site (FI), or alanine-substituted FW motif (FW) mutants. (**B**) Effects of individual slow-site alanine substitutions on *Egr1* expression. Data are expressed relative to expression of GAPDH. In (A) and (B), cells were stimulated with TPA (50 ng/ml) where indicated. RNA levels are quantified relative to GAPDH; data are means ± SEM, $n = 3$. (**C**) Proliferation of wild-type and mutant Elk-1 TKO MEFs. Data are means ± SEM, $n = 3$. (**D**) Coimmunoprecipitation of Mediator with wild-type or mutant Flag-tagged Elk-1 from N H3T3 cell extracts. Antibodies to Mediator subunits MED23, MED24, and MED16 were used for immunoblotting. (**E**) Mediator coprecipitation from unstimulated NIH3T3 cell extracts using wild-type and mutant GST-tagged Elk-1 TAD proteins with and without prior ERK2 phosphorylation.

our results show that the different rates of Elk 1 TAD phosphorylation by ERK2 follow a com petition mechanism that is governed by the po sition of individual Elk 1 substrate sites relative to ERK2 docking interactions.

To test whether the different kinetic classes of Elk 1 TAD phosphorylation sites are function ally equivalent, we expressed Elk 1 mutants in fibroblasts derived from TCF deficient ($Elk1^{-/-}$; $Elk3^{\delta/\delta}$; $Elk4^{-/-}$) triple knockout mouse embryos (TKO MEFs; fig. S4, A to C). In these cells, immediate early (IE) gene expression is defective, but expression of wild type mouse Elk 1 restored the IE transcriptional activation seen in wild type MEFs after activation of ERK by treatment with TPA (12 *O* tetradecanoylphorbol 13 acetate) (fig. S4D). As expected, alanine substitutions of fast and/or intermediate sites, or of the FW motif, greatly diminished or abolished the ability of Elk 1 to activate TCF SRF target gene transcription after TPA stimulation (Fig. 3A). Surprisingly, how ever, mutation of the slow sites substantially en hanced Elk 1 mediated activation of TCF SRF target genes (Fig. 3A). Alanine substitutions at individual slow sites also increased Elk 1 activity, with Thr^{418} exhibiting the greatest effect (Fig. 3B and fig. S4, E to G). TCF SRF signaling is impor tant for cellular proliferation (*26*, *27*), and TKO MEFs proliferated more slowly than wild type MEFs. The reconstituted TKO MEFs exhibited enhanced proliferation rates, which correlated with the ability of each mutant to promote tran scriptional activation (Fig. 3C).

Phosphorylation of Elk 1 promotes transcrip tional activation by facilitating its MED23 dependent interaction with the Mediator complex (*16 18*). We therefore investigated whether the different transcriptional activities of the Elk 1 mutants reflected alterations in Mediator binding. We pre pared extracts of TKO cells expressing wild type or mutant Elk 1 proteins and assessed Elk 1 associa tion with Mediator by coimmunoprecipitation of the MED23, MED24, and MED16 subunits. Con sistent with the transcription experiments, Elk 1 Mediator interaction was induced by TPA stimulation and dependent on the FW motif; it was abolished by alanine substitutions of fast and intermediate sites, and increased in the slow site Elk 1 mutant (Fig. 3D). We obtained similar results when we used glutathione *S* transferase (GST) Elk 1 TAD proteins to recover Mediator proteins from unstimulated NIH3T3 cell extracts (Fig. 3E). In this assay, ERK2 phosphorylation time course experiments showed that Mediator recovery by the wild type Elk 1 TAD was most efficient prior to modifications of the slow sites (fig. S5, A and B). Taken together, these data show that according to the sites involved, ERK2 phosphorylation promotes or inhibits tran scriptional activation by Elk 1, which reflects al terations in Elk 1 Mediator interactions.

Next, we investigated Elk 1 TAD phosphoryla tion kinetics in vivo. Previous studies were un able to distinguish the progressive phosphorylation of fast and slow Elk 1 sites (*6*). However, by in cubating cells at 25°C to slow down reactions, we confirmed that phosphorylation rates can be ranked in the order Ser^{384} > Thr^{364} > Thr^{418} and that different site classes exhibited a similar com petitive behavior, as seen in vitro (fig. S6A). Rea soning that phosphorylation of the Elk 1 TAD might be sensitive to kinetic effects at limiting signal strengths, we titrated ERK activity using

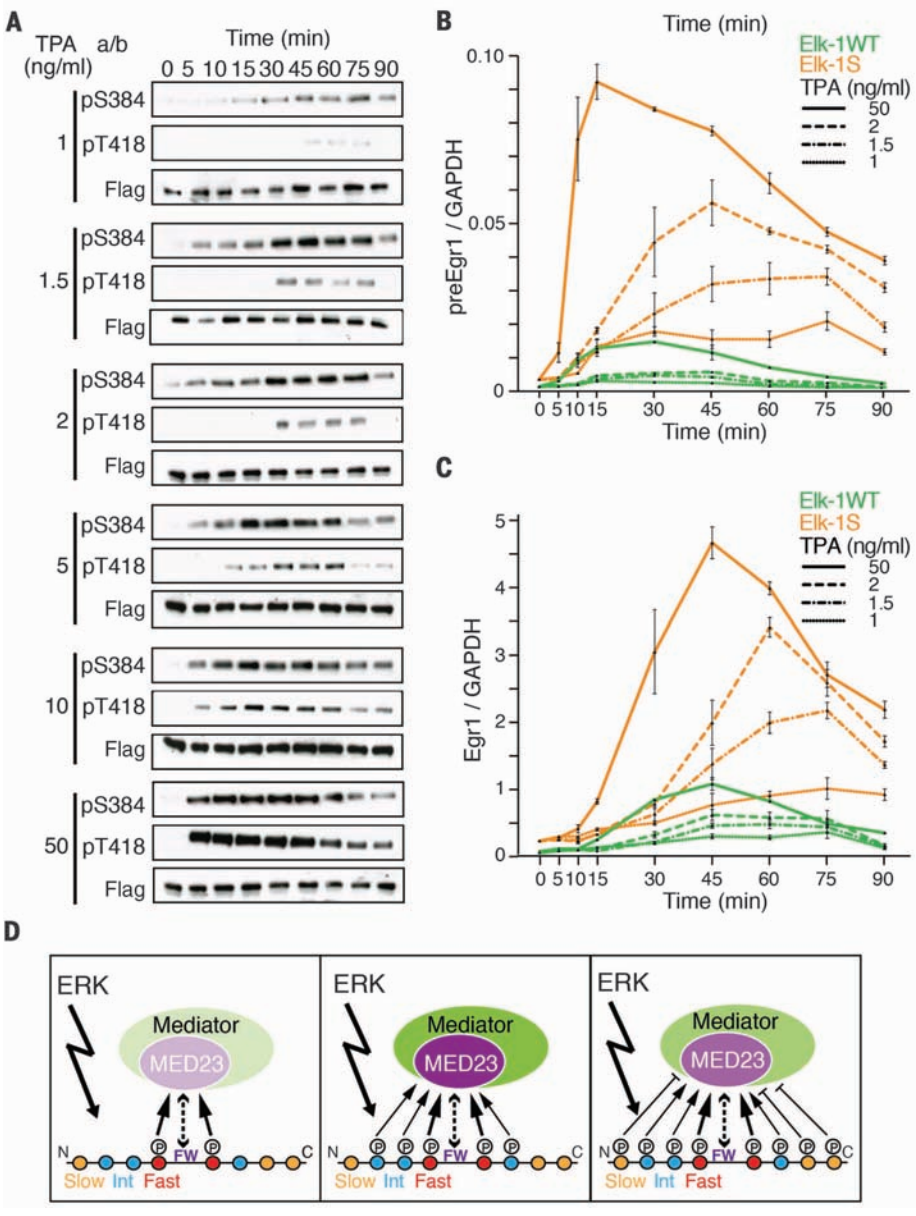

Fig. 4. Multisite phosphorylation of Elk-1 shapes the transcr ptional response to ERK activation. (**A**) Kinetics of Elk-1 fast- and slow-site phosphorylation in cells treated with increasing concentrations of TPA. (**B**) Transcription rate of the TCF-SRF target gene *Egr1* in TKO MEFs expressing wild-type Elk-1 or mutant Elk-1S. Precursor RNA was monitored by qRT-PCR after stimulation with different concentrations of TPA. Data are means ± SEM; $n = 3$. (**C**) Kinetics of *Egr1* mRNA accumulation in cells as in (B) monitored by qRT-PCR. (**D**) Progressive Elk-1 phosphorylation by ERK has both activating (left and center) and inhibitory (right) effects on Mediator recruitment, as suggested by shading densities. A strong signal will rapidly reach the attenuated state shown at the right; a weak signal may reach this state only if sustained.

increasing amounts of TPA. This both increased the maximal extent of ERK activation and advanced the time at which it occurred (fig. S6B). At low TPA concentrations, Elk 1 fast site (Ser^{384}) and slow site (Thr^{418}) modifications accumulated slowly over 1 hour, whereas at a saturating TPA dose they were maximal by 10 min. Both phosphoryl ations declined at late times, presumably owing to the action of Elk 1 phosphatases (Fig. 4A) (*6*, *28*).

Having established that Elk 1 phosphoryla tion kinetics are tuned by signal strength, we investigated their relationship to transcriptional activation. We compared the ability of wild type Elk 1 and the slow site mutant Elk 1S to activate transcription in response to signals of differing strengths. At saturating TPA concentrations, both proteins activated *Egr1* transcription with sim ilar transient kinetics, although Elk 1S was much more active, reflecting the loss of the inhibitory sites (Fig. 4, B and C). At limiting TPA doses, however, their behaviors were markedly different. Whereas the activity of wild type Elk 1 was almost maximal by 15 min, that of Elk 1S increased sub stantially beyond this time (Fig. 4B), resulting in prolonged *Egr1* mRNA accumulation (Fig. 4C). Thus, progressive phosphorylation of the Elk 1 TAD by a single kinase, ERK, attenuates the transcrip tional response of Elk 1, shaping it according to the strength and kinetics of ERK activation.

Our results show that phosphorylation of the Elk 1 TAD by ERK can either promote or inhibit Mediator interaction depending on the sites in volved, thereby modulating transcriptional activa tion. Given that the TAD sequences are conserved in the other TCFs, our findings may also apply to them. The more rapidly phosphorylated sites are located in the substantially conserved central core of the TAD and are essential for transcriptional activation, lying close to the FW hydrophobic motif required for Elk 1 Mediator interaction (*10*, *18*). Multisite phosphorylation of these res idues might stabilize this interaction and per haps also set a signaling threshold for it, similar to the way that multisite phosphorylation sets a threshold for the Sic1 Cdc4 interaction (*29*). In contrast, slowly phosphorylated sites located N and C terminal of the conserved TAD core act negatively. Their phosphorylation inhibits Mediator recruitment and limits transcriptional activation (Fig. 4D) and may also facilitate recruitment of negative regulators of Elk 1 activity. Together, these properties ensure that ERK phosphorylation of the Elk 1 TAD is self limiting, whereby phospho rylation of slow sites attenuates TCF SRF target gene expression under conditions of strong or sustained ERK signaling (Fig. 4D). Our results challenge the common assumption that multisite modification events act unidirectionally and can only be reversed or limited by antagonistic enzymes, such as phosphatases. Given the prevalence of such events in different biological processes, we expect that similar mechanisms may govern other reg ulatory interactions.

REFERENCES AND NOTES

1. J. Gunawardena, *Proc. Natl. Acad. Sci. U.S.A.* **102**, 14617 14622 (2005).
2. J. Gunawardena, *Biophys. J.* **93**, 3828 3834 (2007).
3. C. Salazar, T. Höfer, *FEBS J.* **276**, 3177 3198 (2009).
4. X. Liu, L. Bardwell, Q. Nie, *Biophys. J.* **98**, 1396 1407 (2010).
5. M. Karin, T. Hunter, *Curr. Biol.* **5**, 747 757 (1995).
6. F. H. Cruzalegui, E. Cano, R. Treisman, *Oncogene* **18**, 7948 7957 (1999).
7. R. Janknecht, W. H. Ernst, V. Pingoud, A. Nordheim, *EMBO J.* **12**, 5097 5104 (1993).
8. R. Marais, J. Wynne, R. Treisman, *Cell* **73**, 381 393 (1993).
9. R. Janknecht, W. H. Ernst, A. Nordheim, *Oncogene* **10**, 1209 1216 (1995).
10. M. A. Price, A. E. Rogers, R. Treisman, *EMBO J.* **14**, 2589 2601 (1995).
11. H. Gille *et al.*, *EMBO J.* **14**, 951 962 (1995).
12. D. A. Fantz, D. Jacobs, D. Glossip, K. Kornfeld, *J. Biol. Chem.* **276**, 27256 27265 (2001).
13. S. H. Yang, P. R. Yates, A. J. Whitmarsh, R. J. Davis, A. D. Sharrocks, *Mol. Cell. Biol.* **18**, 710 720 (1998).
14. S. H. Yang, A. J. Whitmarsh, R. J. Davis, A. D. Sharrocks, *EMBO J.* **17**, 1740 1749 (1998).
15. D. Jacobs, D. Glossip, H. Xing, A. J. Muslin, K. Kornfeld, *Genes Dev.* **13**, 163 175 (1999).
16. J. L. Stevens *et al.*, *Science* **296**, 755 758 (2002).
17. G. Wang *et al.*, *Mol. Cell* **17**, 683 694 (2005).
18. M. A. Balamotis *et al.*, *Sci. Signal.* **2**, ra20 (2009).

19. W. Wang *et al*., *Dev. Cell* **16**, 764 771 (2009).
20. F. X. Theillet *et al*., *Nat. Protoc.* **8**, 1416 1432 (2013).
21. M. Cavigelli, F. Dolfi, F. X. Claret, M. Karin, *EMBO J.* **14**, 5957 5964 (1995).
22. H. Gille, T. Strahl, P. E. Shaw, *Curr. Biol.* **5**, 1191 1200 (1995).
23. A. J. Whitmarsh, P. Shore, A. D. Sharrocks, R. J. Davis, *Science* **269**, 403 407 (1995).
24. M. A. Price, F. H. Cruzalegui, R. Treisman, *EMBO J.* **15**, 6552 6563 (1996).
25. D. L. Sheridan, Y. Kong, S. A. Parker, K. N. Dalby, B. E. Turk, *J. Biol. Chem.* **283**, 19511 19520 (2008).
26. E. R. Vickers *et al*., *Mol. Cell. Biol.* **24**, 10340 10351 (2004).
27. M. A. Wozniak *et al*., *Curr. Biol.* **22**, 2017 2026 (2012).
28. T. Sugimoto, S. Stewart, K. L. Guan, *J. Biol. Chem.* **272**, 29415 29418 (1997).
29. P. Nash *et al*., *Nature* **414**, 514 521 (2001).

ACKNOWLEDGMENTS

Work in the Treisman group was supported by the Francis Crick Institute, which receives its core funding from Cancer Research UK (FC001 190), the UK Medical Research Council (FC001 190), and the Wellcome Trust (FC001 190), and by European Research Council (ERC) advanced grant 268690 ACTINonSRF. Work in the Selenko group is funded by ERC consolidator grant 647474 NeuroInCellNMR. F. X.T. is supported by Agence Nationale pour la Recherche grant ANR14 ACHN 0015 01. The authors have no conflicts of interest. Author contributions: A.M. conceived the project; A.M., C.F., and F.M. designed and performed molecular and cell biology experiments; F. X.T., T.M.C., and P.A.B. developed the competitive inhibition model; F. X.T. and P.S. designed, executed, and interpreted the NMR experiments; and A.M., P.S., and R.T. designed and interpreted experiments and wrote the paper. We thank F. Gualdrini, C. Esnault, and P. Costello for characterizing gene regulation in reconstituted TKO MEFs, sharing their unpublished data, and generating reconstituted TKO MEF cells; the Crick Genomics and Flow Cytometry technology platforms for technical support; and A. Behrens, V. Calleja, A. Chakraborty, M. Diefenbacher, C. Duellberg, R. Nicolas, P. Riou, M. Skehel, and our group members for advice and discussions.

SUPPLEMENTARY MATERIALS

www.sciencemag.org/content/354/6309/233/suppl/DC1
Figs. S1 to S6
References (*30* *41*)

5 August 2015; accepted 23 August 2016
10.1126/science.aad1872

VACCINES

Rapid development of a DNA vaccine for Zika virus

Kimberly A. Dowd,[1]* Sung Youl Ko,[2]* Kaitlyn M. Morabito,[2] Eun Sung Yang,[2] Rebecca S. Pelc,[1] Christina R. DeMaso,[1] Leda R. Castilho,[2,3] Peter Abbink,[4] Michael Boyd,[4] Ramya Nityanandam,[4] David N. Gordon,[1] John Robert Gallagher,[5] Xuejun Chen,[2] John Paul Todd,[2] Yaroslav Tsybovsky,[6] Audray Harris,[5] Yan Jang S. Huang,[7] Stephen Higgs,[7] Dana L. Vanlandingham,[7] Hanne Andersen,[8] Mark G. Lewis,[8] Rafael De La Barrera,[9] Kenneth H. Eckels,[9] Richard G. Jarman,[10] Martha C. Nason,[11] Dan H. Barouch,[4] Mario Roederer,[2] Wing Pui Kong,[2] John R. Mascola,[2] Theodore C. Pierson,[1]† Barney S. Graham[2]†

Zika virus (ZIKV) was identified as a cause of congenital disease during the explosive outbreak in the Americas and Caribbean that began in 2015. Because of the ongoing fetal risk from endemic disease and travel-related exposures, a vaccine to prevent viremia in women of childbearing age and their partners is imperative. We found that vaccination with DNA expressing the premembrane and envelope proteins of ZIKV was immunogenic in mice and nonhuman primates, and protection against viremia after ZIKV challenge correlated with serum neutralizing activity. These data not only indicate that DNA vaccination could be a successful approach to protect against ZIKV infection, but also suggest a protective threshold of vaccine-induced neutralizing activity that prevents viremia after acute infection.

The emergence of Zika virus (ZIKV) in the Americas and Caribbean follows a series of global threats to public health from mosquito borne viral diseases over the past three decades. Because of the profound impact on individuals and society from a disabling congenital disease caused by ZIKV infection in pregnant women, the World Health Organization declared ZIKV a global health emergency in February 2016. Although it is likely that the incidence of ZIKV infection will decline considerably within 1 to 2 years (*1*), it is also likely that ZIKV will become endemic in tropical and subtropical regions, with sporadic outbreaks and potential for spread into new geographical areas, as observed with other emerging arboviruses such as West Nile (WNV) and chikungunya. Therefore, unless immunity is established before childbearing age, pregnant women will continue to be at risk for an infection that could harm their fetus. Further, because men can harbor ZIKV in semen for several months after a clinically unapparent infection and can sexually transmit virus to a pregnant partner (*2*), even women in nonendemic regions will have some ongoing risk if exposed to men who have traveled to endemic regions. These characteristic features of transmission and disease suggest that there will be an ongoing need for a ZIKV vaccine to maintain a high level of immunity in the general population and in travelers to endemic regions to reduce the frequency of fetal infection.

To rapidly address the critical need for a preventive vaccine to curtail the ongoing ZIKV outbreak in the Americas, we chose a gene based vaccine delivery approach that leverages our prior experience with a DNA based WNV vaccine (*3*). Advantages of DNA vaccines include the ability to rapidly test multiple candidate antigen designs, the ability to rapidly produce material that conforms to good manufacturing practices, an established safety profile in humans, and a relatively straightforward regulatory pathway into clinical evaluation.

Antigen design was guided by prior knowledge about humoral immunity to flaviviruses. Vaccine elicited neutralizing antibodies (NAbs) are associated with protection from flavivirus mediated disease (*4*). Because the most potent monoclonal flavivirus NAbs map to conformational epitopes in domain III (DIII) of the envelope (E) protein (*5*), or to more complex quaternary epitopes that bridge between antiparallel E dimers or between dimer rafts arrayed on the virus surface (*6*, *7*), our goal was to identify constructs that produced particles that faithfully captured the antigenic complexity of infectious virions. Expression of the structural proteins premembrane (prM) and E are sufficient for the production and release of virus like subviral particles (SVPs) with antigenic and functional properties similar to those of infectious virions (*8*, *9*).

To identify promising vaccine candidates, prM E constructs were synthesized and screened for expression and efficiency of particle release from transfected cells. prM E sequences were inserted into a cytomegalovirus immediate early promoter containing vector (VRC8400) that has been evaluated clinically in several previous studies (*3*, *10*, *11*). These constructs are distinct from one reported in recent studies by Larocca *et al*. (*12*) and Abbink *et al*. (*13*) that was based on a Brazilian isolate (strain

[1]Viral Pathogenesis Section, National Institute of Allergy and Infectious Diseases, National Institutes of Health, Bethesda, MD 20892, USA. [2]Vaccine Research Center, National Institute of Allergy and Infectious Diseases, National Institutes of Health, Bethesda, MD 20892, USA. [3]Federal University of Rio de Janeiro, COPPE (Instituto Alberto Luiz Coimbra de Pós Graduação e Pesquisa de Engenharia), Chemical Engineering Program, Rio de Janeiro, Rio de Janeiro, Brazil. [4]Center for Virology and Vaccine Research, Beth Israel Deaconess Medical Center, Harvard Medical School, Boston, MA 02215, USA. [5]Structural Informatics Unit, Laboratory of Infectious Diseases, National Institute of Allergy and Infectious Diseases, National Institutes of Health, Bethesda, MD 20892, USA. [6]Electron Microscopy Laboratory, Cancer Research Technology Program, Leidos Biomedical Research, Frederick National Laboratory for Cancer Research, Frederick, MD 21702, USA. [7]Department of Diagnostic Medicine/Pathobiology, College of Veterinary Medicine, Kansas State University, Manhattan, KS 66506, USA. [8]Bioqual, Rockville, MD 20852, USA. [9]Translational Medicine Branch, Walter Reed Army Institute of Research, Silver Spring, MD 20910, USA. [10]Viral Diseases Branch, Walter Reed Army Institute of Research, Silver Spring, MD 20910, USA. [11]Biostatistics Research Branch, Division of Clinical Research, National Institute of Allergy and Infectious Diseases, National Institutes of Health, Bethesda, MD 20852, USA.
*These authors contributed equally to this work. **†Corresponding author. Email: piersontc@niaid.nih.gov (T.C.P.); bgraham@mail.nih.gov (B.S.G.)**